Asian Journal of Chemistry; Vol. 36, No. 2 (2024), 307-316

ASIAN JOURNAL OF CHEMISTRY

https://doi.org/10.14233/ajchem.2024.30711

Mechanical Properties, Morphological Characterization and Melt Dripping Studies of Polypropylene (PP) + High Density Polyethylene (HDPE) + Polystyrene (PS) Ternary Polymer Blends: Non-Isothermal Degradation Kinetics of Compatibilized and Uncompatibilized Blends

C. Surej Rajan[1], Lity Alen Varghese[1,*], Shiny Joseph[1] and Soney C. George[2]

[1]Department of Chemical Engineering, National Institute of Technology Calicut, Kozhikode-673601, India
[2]Centre for Nanoscience and Technology, Amal Jyothi College of Engineering, Kanjirapilly-686518, India

*Corresponding author: E-mail: lityalen@nitc.ac.in

Received: 15 October 2023; *Accepted*: 19 November 2023; *Published online*: 31 January 2024; AJC-21517

Polymer composites have been widely used due to its light weight, performance with good mechanical properties, corrosion resistant, solvent resistance and it becomes an important part of the industries. Polypropylene (PP), polystyrene (PS) and high-density polyethylene (HDPE) are applied to various commercial as well as automobile spare parts. In this study PP, PS and HDPE were melt mixed together to form a ternary polymer blend and mechanical, morphological, thermogravimetric analysis were conducted to determine its potential applications. The compatibilization of the blend was achieved by the combination of ethylene-propylenediene-monomer (EPDM) and styrene-ethylene-butylene-styrene (SEBS). Model free methods like Flynn Wall Ozawa (FWO), Kissinger-Akahira-Sunose equation (KAS) and Friedman methods were applied to estimate the activation energy values at different heating rates of 5, 10 and 15 ºC/min. The compatibilized blend of 80PP/5PS/15HDPE with 5% SEBS/EPDM showed better tensile strength compared to uncompatibilized. Freidman method produced a higher value of average activation energy as 203.4 kJ/mol. The melt dripping characteristics was also analyzed were the time to ignition and time for first drip was found to be in the range of 6 to 9 s and 14-16 s. Pure and compatibilized blends showed a very low limiting oxygen index (LOI) values as in the range of 18.7 to 18.9. Elastomeric/rubber blend compatibilization was achieved and the material can be applied to light weight automobile applications. From morphological characterization, it was understood that compatibilized blends are more durable and easily transfer the stress uniformly through the interface. This compatibilized blend can also be used in low temperature regions.

Keywords: Polypropylene, Polystyrene, High density polyethylene, Compatibilizer, Polymer blends.

INTRODUCTION

Due to their high molecular masses, polymer blends are largely immiscible at the molecular level. The structure formed during the production of the polymer blends has a significant impact on their characteristics. In order to obtain the desired final material properties, compatibilization can be achieved by lowering the interfacial tension, reducing the dispersed phase size, preventing both dynamic and static coalescence processes, improving phase adhesion, stabilizing the microstructure and allowing much greater control over the processing conditions. A copolymer that is mixable or highly compatible with either phase can be added to increase miscibility. Blends of polypropylene (PP) and polystyrene (PS) are best suited for creating low performance components like computer casings, dashboards, *etc.* [1].

Pyrolysis is a superior alternative to recover energy from plastics beyond the goods' shelf lives as chemicals and fuels because of its low operating temperature and clean products [2]. Pyrolysis is also commonly associated to the production of valuable tars with yields between 75 and 80 wt.% at comparatively low temperatures between 500 and 650 ºC. Because pyrolysis uses an inert atmosphere devoid of oxygen and has higher environmental benefits, it does not produce dioxins (notorious anthropogenic environmental toxicants) when its products react with oxygen. Through a reduction in carbon dioxide and carbon monoxide emissions, this technique also lowers the carbon footprint of products and processes [3]. The

process of thermal degradation of plastics is complicated in nature. The conversion of post-consumer thermoplastics depends significantly on the pyrolysis process's kinetics and the accompanying the iso-conversional models [4].

Ternary blends allow for the formation of three different sorts of component interactions. The addition of the compatibilizers, which alters the interfacial tension, can modify the kind of phase structure. The blend composition mostly determines the kind of phase structure. The impact strength was significantly increased by the addition of styrene butadiene styrene (SBS) and styrene ethylene/butene styrene (SEBS) copolymer. Impact strength values and the morphology of PP/HDPE/SBS-SEBS blends were highly dependent on the circumstances surrounding their mixing. The effectiveness of these compatibilizers is influenced by their molecular properties, which in turn are affected by the composition and properties of blends [5].

The degree of dispersion was enhanced by increasing the mixing duration and intensity, but prolonged or vigorous mixing also increased thermal and mechanical deterioration. Therefore, for improved results, an ideal mixing process should be needed [6]. The addition of SEBS resulted in enhanced tensile and impact characteristics, as well as increased elongation at break and ductility. At the same time as strength and modulus were decreased, the copolymer concentration showed an improvement in ductility, toughness and impact characteristics [7]. In the ternary system, the main polymer component creates the matrix, which is then filled with two minor phases. The relative spread-ability of the polymer components in a ternary blend determines the morphology of the mixture. The morphology of the ternary polymer blends is also influenced by the processing conditions. Due to local burning, particularly at hot areas in the extruder barrel that alter the mechanical characteristics of the blend, high temperatures may accelerate the deterioration behaviour of some blend components [8].

In order to prevent polystyrene (PS) from coalescing to form bigger domains with a corresponding adjustment in their quantity, the number of scattered PS globules must grow while maintaining a relatively constant diameter. Polystyrene (PS) has a higher density when compared to polyethylene (PE) and polypropylene (PP). The characteristics of the whole matrix are definitely altered by an increase in PS concentration relative to PP or PE [9].

The degradation rate of PS was not significantly affected, however, the degradation rate of polyethylene was increased during the binary degradation at 440 ºC. The PS radicals extracted hydrogen from PE, which accelerated the breakdown of PE. The total degradation rates of the PS/PP binary combination were higher than the sum of the individual component degradation rates. According to certain experimental studies, binary degradation of PS and PP increased the rate of PP degradation at various temperatures while keeping the rate of PS degradation constant. In this case, the low molecular weight radicals removed hydrogen from PP as they penetrated the substance, so accelerating the degradation of polymer [10].

The kinetics of pyrolysis is the most crucial piece of knowledge when designing a plastic breakdown process. The foundation of model-free techniques is a plot based on the degradation temperature at different heating rates. These strategies necessitate data from diverse heating rates but produce no understanding of response rate laws [11]. Polymer composites with polypropylene (PP), polystyrene (PS) and high density polyethylene (HDPE) and their binary blends were extensively studied for various applications. To improve the interfacial adherence and unform transfer of stress, compatibilizer combination of ethylene-propylene-diene-monomer (EPDM) and styrene-ethylene-butylene-styrene (SEBS) were analyzed. The mechanical characteristics of the compatibilized ternary polymer blends were examined in this study. In addition, the compatibilized and uncompatibilized blends are subjected to a kinetic analysis of the thermogravimetric (TGA) data under pyrolysis circumstances (non-oxidizing condition) at four different heating speeds. Model-free approaches were used to estimate the kinetic parameter. The fundamental studies on the flammability of the thermoplastic ternary polymer blend were also discussed.

EXPERIMENTAL

The materials were homopolymer polypropylene (H110MA), M/s Reliance Industries Ltd., India melt flow index (MFI) 11 g/10 min (ASTM D1238, 230 ºC/2.16 kg); high density polyethylene (HDPE) (HD50MA180) from Reliance Industries Ltd., India with an MFI 20 g/10 min (ASTM D1238, 190 ºC/2.16 kg). Polystyrene (PS) was obtained from Supreme Petrochem Ltd.-MFI 12 g/10 min (ASTM D1238, 200 ºC/5 kg). Styrene-ethylene-butadiene-styrene (SEBS)/polystyrene-block-poly-(ethylene-ran-butylene)-block-polystyrene powder, average M_w ~118,000 by GPC, contains > 0.03% antioxidant as inhibitor purchased from Sigma-Aldrich and ethylene propylenediene monomer (EPDM) from Popular Rubber Products, Kochi, India.

Preparation of polymer blend: The polymer blends and composites were melt mixed as per the formulation given in Table-1 using a thermo-Haake Rheocord equipped with twin screw rollers. For the preparation of the ternary polymer blends, PP/PS/HDPE were blended at 180 ºC with a rotational speed of 45 rpm for 8 min. The compatibilizers such as styrene ethylene butadiene styrene (SEBS) and ethylene propylenediene monomer (EPDM) were added after 2 min mixing of polymer blend. In this preparation, the polymer blend composition of PP/PS/HDPE was fixed as 80/5/15 followed with SEBS and EPDM composition ranges from 5 wt.% to 25 wt.%.

TABLE-1
COMPATIBILIZER COMPOSITION SEBS/EPDM

Sample	SEBS (%)	EPDM (%)
80PP/5PS/15HDPE	5	5
	10	10
	15	15
	20	20
	25	25

Characterization: The tensile properties (ASTM D638) of pure and compatibilized ternary polymer blend were characterized using Shimadzu Autograph Universal Testing Machine (UTM) as per the ASTM standards. The thermal stability of the composites was determined using TGA-DTA Hitachi STA7000 at a heating rate of 5, 10 and 15 ºC/min. To study the kinetics

of compatibilized plastic decomposition process same heating rates were used under the presence of nitrogen. A Jeol 6390LA/ OXFORD XMX N instrument was used for the surface morphology analysis. Melting and crystallization characteristics of the polymer composites were analyzed using DSC Netzsch DSC 204 F1 Heat flux DSC. The crystallinity of the samples was analyzed with X-Ray Diffraction using Bruker D8 Advance. The functional groups present in the composites were analyzed with Perkin-Elmer FTIR in the range of 4000-400 cm^{-1}.

Kinetic studies: There are two major methods *viz*. model fitting and model free method, which are employed for the decomposition of solids. Model free methods does not have any previous assumptions about the reaction model and allows the kinetic parameters to be calculated as a function of the conversion degree. Different model free method such as Friedman, Flynn wall Ozawa (FWO), Kissinger-Akahira-Sunose equation (KAS) have been proposed and used for the kinetic study of solid materials.

The reaction rate ($d\alpha/dt$) of the pyrolysis of material can be expressed as follows:

$$\frac{d\alpha}{dt} = K(T).f(\alpha) \quad (1)$$

$$\alpha = \frac{w_o - w}{w_i - w_f} \quad (2)$$

where α is the reaction conversion and t the time in min; K is the reaction rate constant (K^{-1}) as expressed as $K(T) = A \exp(-E_a/RT)$; A is the pre-exponential factor; E_a is activation energy; R is Universal gas constant (8.314 J mol^{-1} K^{-1}); T is temperature (K); w_o is initial weight of the sample used for the experiment; w is instantaneous weight of the sample (at time t); and w_f is weight left of the sample at the end of the experiment.

For the non-isothermal pyrolysis, the heating rate (β) can be defined as $\beta = dT/dt$ and thus the reaction rate can be written as:

$$\beta\frac{d\alpha}{dt} = A\exp\left(\frac{-E_a}{RT}\right)f(\alpha)$$

One of the differential techniques that is most used in the equal conversion thermal analysis method, which is the simplest method to determine the activation energy, is the Friedman method. The KAS Akahira-Sunose (KAS) equation is a differential method that depends on the conversion rate and temperature and delivers a considerable improvement in the accuracy of activation energy estimations. A minimum of three heating rates must be obtained in order to use this equation, with the corresponding conversion curves being assessed from the observed TG curves. The plot of $\ln(\beta/T^2)$ against (1/T) for each conversion should result in a straight line with a slope precisely proportional to activation enThe Flynn-Wall-Ozawa (FWO) technique is a "model-free" approach that states that the conversion function $f(\alpha)$ remains constant for all values of, as the heating rate changes. In this approach, the experiments at different heating rates were used to measure the temperatures which correspond to the fixed values of α [12,13].

Friedman method:

$$\ln\left(\beta\frac{d\alpha}{dt}\right) = \ln\left(A.\left(f(\alpha)\right)\right) - \frac{E_a}{RT} \quad (3)$$

FWO method:

$$\ln(\beta) = \ln\frac{A.E_a}{R.g(\alpha)} - 5.331 - 1.052\frac{E_a}{RT} \quad (4)$$

KAS method:

$$\ln\frac{\beta}{T^2} = \ln\frac{A.R}{E_a.g(\alpha)} - \frac{E_a}{RT} \quad (5)$$

Melt dripping studies: The burning behaviour of the UL94-specimens injection moulded from the extruded compounds was examined during the UL94 standard test. Typically, the specimen was burned for 10 s before the fire was extinguished after the specimen begins to differentiate. The compound performs best and is categorized as V-0 if the specimen burns for a total of 50 s without producing burning drops and only for a maximum of 10 s within that time. After one flame treatment, if the specimen burns for up to 30 s without leaking and with the remaining specimen, it achieves V-1. The specimen achieves V-2 if burning droplets form but the specimen is not completely burned and the burning time is under 30 s. The specimen failed or was not categorized if it burned for a longer period of time or left no residual specimen [14]. Under the UL 94 vertical burning test circumstances, two categories were specified Type I: tiny and uniform drop size with short initial dripping time and type II: big and irregular drop size with extended first dripping time. Regarding the variables affecting the dripping, it was considered that the dripping was caused by a decrease in viscosity brought on by both physical melting and chemical deterioration. End chain scission's decomposition process would correlate to bulk softening and large-scale dripping, whereas random chain scission's decomposition mechanism tended to result in surface melting and small-scale dripping. Under the UL 94 test conditions, the materials that appeared to predominate the dripping types of polymers had key qualities such as the activation energy of viscous flow and the ratio of the effective heat of combustion to the heat of gasification [15,16].

According to ASTM D 2863, the limiting oxygen index (LOI) test was also conducted. During the test, the flow of oxygen and nitrogen were managed while the sample was held vertically in the clear chimney. To find the lowest oxygen concentration required to burn the sample in 3 min, the test was repeated under different nitrogen and oxygen concentrations.

RESULTS AND DISCUSSION

FTIR studies: The FTIR spectra of uncompatibilized and compatibilized ternary polymer blends are shown in Fig. 1. All the functional groups present in PP/HDPE/PS blends with SEBS and EPDM were found with the corresponding wavenumber in the spectrum. The main functional groups with their corresponding wavenumbers are shown in Table-2 [17,18].

XRD studies: The crystalline characteristics of the pure and compatibilized ternary polymer blends were analyzed using XRD technique. Fig. 2 shows the diffraction peaks of both

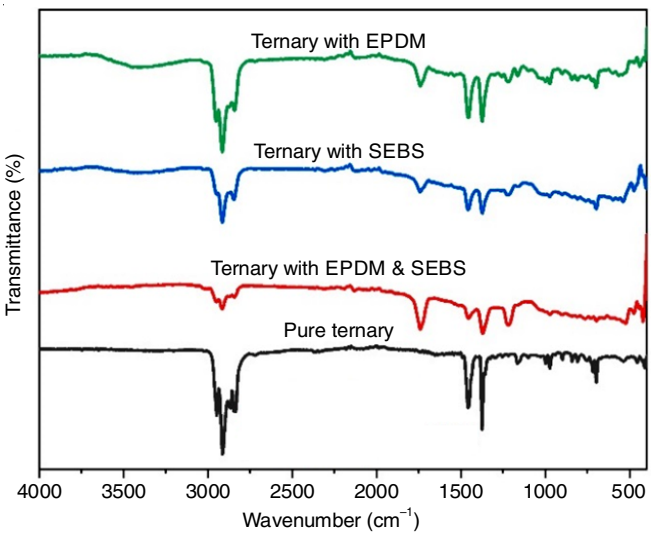

Fig. 1. FTIR spectrum of polymer blends

TABLE-2
FUNCTIONAL GROUPS IN THE POLYMER BLEND

Wavenumber (cm^{-1})	Functional group
2946	C-H stretching
2918	CH_3 asymmetric stretching vibration
2844	CH_2 symmetric stretching
1740	C=C bending
1685	C=C stretching
1462	CH_2 symmetric bending
1374	CH_3 symmetric bending
980	CH_3 rocking bibration
705	C-H bending

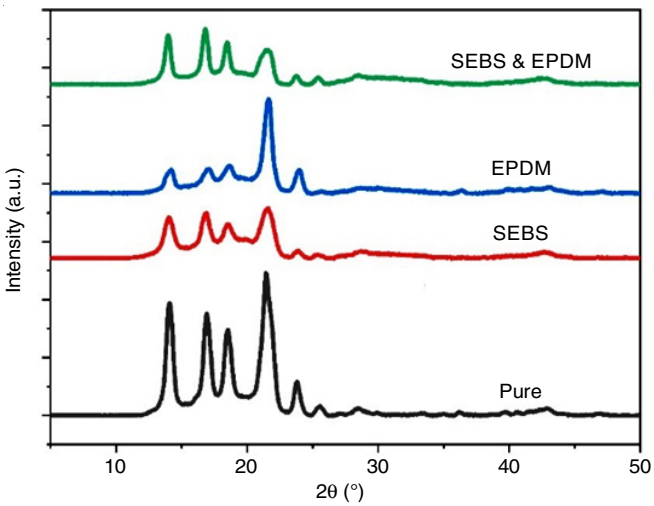

Fig. 2. XRD of polymer blends

uncompatibilized and compatibilized ternary polymer blend. Pure PP shows the diffraction peaks at 2θ values of 14.28º, 17.14º and 18.92º which corresponds to 110, 040 and 130 planes, respectively of monoclinic α-form. The peaks observed at 110 and 200 depicts the orthorhombic crystals of HDPE at 21.6º and 24.1º [17,19]. Neat PS produces amorphous broad peak in the range of 15-22º. Pure ternary polymer blend exhibits diffraction peaks at corresponding 2θ values of PP, HDPE and PS, showing the presence of all the components in the ternary blend. Compatibilized ternary blend also possess the diffraction peaks at the same angle, confirming the presence of compatibilizers (SEBS & EPDM) in the compatibilized ternary polymer blend. Table-3 shows the effect of compatibilizer addition on the crystallinity of ternary polymer blend. It was found that the percentage crystallinity of polymer blends was decreased upon the addition of SEBS and EPDM into the ternary polymer matrix. This can be due to the addition of amorphous natured compatibilizers into the crystalline matrix. The percentage crystallinity was decrease 42% and 31% increase in the amorphous nature was observed upon compatibilizer addition [20].

TABLE-3
CRYSTALLINITY FROM XRD

	Pure ternary blend	SEBS	EPDM	SEBS & EPDM
Crystallinity (%)	42.2	26.8	24.9	24.1
Amorphous (%)	57.8	73.2	75.1	75.9

Mechanical properties

Tensile strength: In comparison to pure blend, the compatibilized ternary polymer blend's tensile strength resulted in a value of 34.95 MPa. Based on the experiment, the critical compatibilizer concentration for SEBS-EPDM (SE) was 5 wt.% (SE). The combined form of compatibilizer shows a significant improvement in tensile strength of the blend (Fig. 3). According to the literature, EPDM-MA included matrix clearly reduced the tensile strength of PP/HDPE blends [21]. In PP, HDPE exhibits an elastic behaviour that reduces the tensile strength of matrix. The optimum composition of 20/80 HDPE/PP matrix can bear the maximum load at a specific applied load [22]. However, the inclusion of high molecular weight SEBS had a minimal impact on the tensile strength of blend [23]. When a compatibilizer is used in the minimal amount, it locates at the interfacial region and increases the interfacial adhesion. The critical compatibilizer content might reduce the interfacial tension and inhibit droplet coalescence during mixing by being added to

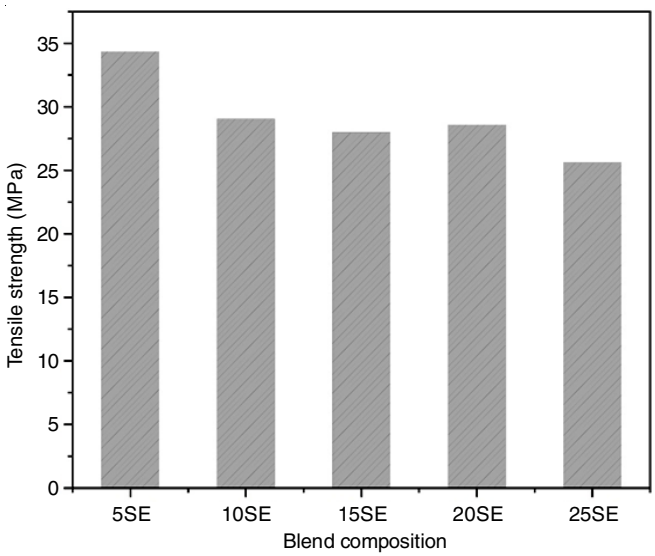

Fig. 3. Tensile strength of polymer blends

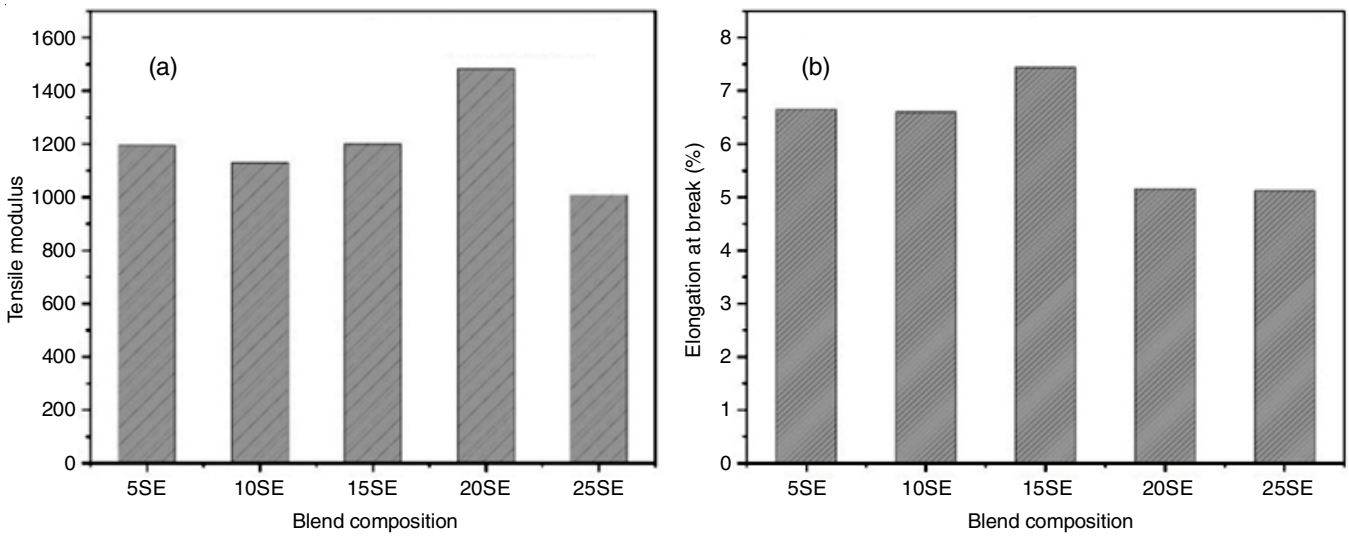

Fig. 4. Tensile modulus (a) and Elongation at break (b) of polymer blends

the polymer matrix. This results in the lack of holes and pullout structure in the compatibilized blends, indicating a significant improvement in the interfacial adhesion of PP/PS [24]. Tensile strength for the uncompatibilized mix is 32.05 MPa. In this case, the SEBS-EPDM compatibilizer mixture performed well inside the polymer matrix and the interfacial adhesion was improved by the critical compatibilizer level content of 5 wt.%, which was effectively dispersed across the interfacial area.

Tensile modulus and elongation at break: The tensile modulus and elongation of break is shown in Fig. 4a-b. The elongation at break is increased on the addition of SEBS to the polymer blend and the trend indicates an improvement in behaviour up to 20% of SEBS-EPDM(SE) blended polymer. The lower percentage of SEBS-EPDM agglomeration in some of the locations of mix may have contributed to the subsequent deterioration of properties. The increased adhesion between the interfaces clearly demonstrates that compatibilized ternary mix had an elongation at break value of 7.45% for a 15 wt.% blend. The behaviour of the tensile modulus changes as the amount of SEBS-EPDM mix increases. In this instance, the addition of 20 wt.% of SEBS-EPDM(SE) blended polymer composites resulted in an 11% increase in tensile modulus. Parameswaranpillai *et al.* [23] claimed that when SEBS is added to the PP/PS blends, the elongation at break increases linearly. It is quite evident that adding 20 wt.% of SEBS to 80/20 PP/PS blends causes a dramatic decrease in elongation at break. While the propylene blocks of EPDM have a great affinity for PP phase, its ethylene blocks have a strong attraction for the HDPE phase. During the melt mixing, EPDM has a greater propensity to migrate to the interface, since EPDM has a low modulus, the tensile modulus lowers [25].

Impact strength: Impact strength of the polymer blends is depicted in Fig. 5. With the addition of SEBS-EPDM to the mix up to 20 SEBS-EPDM compatible blend, the impact strength increases. Further, the addition of SEBS-EPDM decreases the impact strength. This decrease may be the result of the compatibilizer particles adhering in a specific location of the mix, causing the tension to be transferred unevenly across the surface

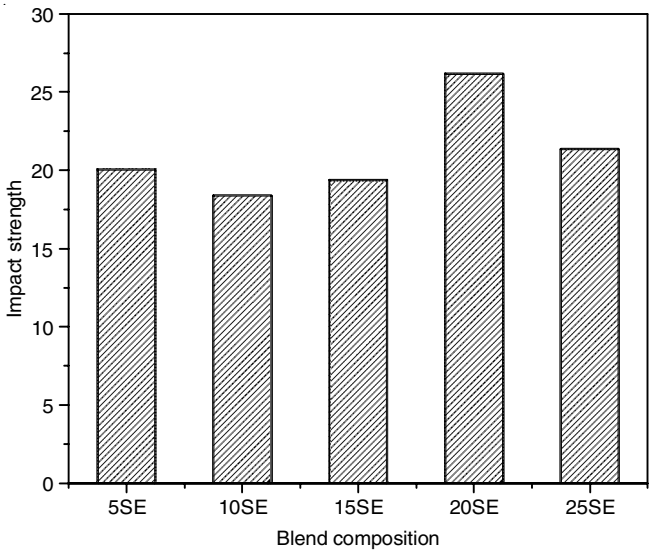

Fig. 5. Impact strength of polymer blends

matrix. In this investigation, the compatibilized blend impact strength was found to be 7% higher than that of pure ternary polymer blend. This undoubtedly expands the applications for the compatibilized blends to lighter ones [21,23].

Kinetics studies: As previously indicated, the Friedman, Flynn-Wall-Ozawa (FWO) Method and Kissinger-Akahira-Sunose (KAS) Method have been used to do kinetic analysis. Fig. 6 represents each model evaluated for pure blend and the blends with SEBS and EPDM.

The kinetic characteristics of several specimens have been investigated using all conversion ranges ($0.1 \geq \alpha \leq 0.9$) and heating rates (β = 5 ºC/min, 10 ºC/min, 15 ºC/min) therefore determining the variation of activation energy with conversion. As stated in Tables 4 and 5, the correlation coefficients (R^2) fall between 0.9 and 0.99, which shows that conversion values have an impact on activation energy. In order to demonstrate the complexity of several reactions, the activation energy values were calculated as a function of reaction conversion. The values of activation energy increase together with the conversion. In

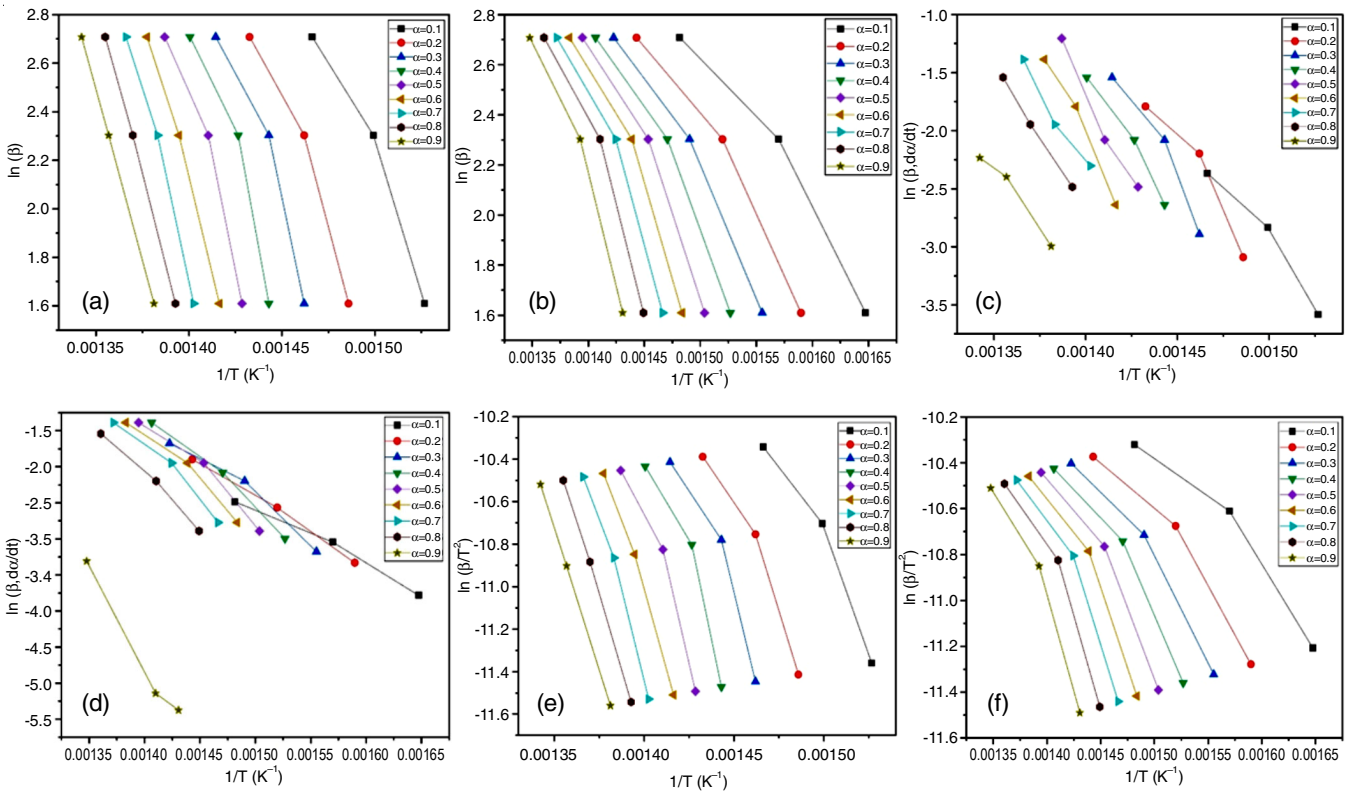

Fig. 6. Flynn-Wall-Ozawa (FWO) method (a & b), Friedman's method (c & d) and Kissinger-Akahira-Sunose (KAS) method (e & f) of pure blend and the blend with SEBS and EPDM

TABLE-4
KINETIC STUDY OF PURE BLEND

Conversion	Differential method		Integral method				Average values	
	Friedman method		FWO method		KAS method			
	E_a (kJ/mol)	R^2	E_a (kJ/mol)	R^2	E_a (kJ/mol)	R^2	E_a (kJ/mol)	R^2
0.1	165.6735	0.9961	142.1125	0.9595	138.3861	0.9585	148.72	0.959
0.2	199.6898	0.9968	161.1323	0.9570	158.1117	0.9560	172.99	0.956
0.3	229.671	0.9991	176.9478	0.9451	174.5755	0.9440	193.73	0.944
0.4	211.3762	0.9976	197.2764	0.9540	195.8326	0.9530	201.49	0.953
0.5	258.5455	0.9970	205.2019	0.9727	204.0563	0.9719	222.60	0.972
0.6	269.3341	0.9583	223.7546	0.9964	223.4888	0.9961	238.85	0.996
0.7	207.9469	0.9677	239.522	0.9928	239.9665	0.9924	229.14	0.992
0.8	206.9939	0.9446	230.8169	0.9992	230.7212	0.9991	222.84	0.999
0.9	166.9901	0.9447	223.1938	0.9992	222.595	0.9991	204.52	0.999
Average	212.91	0.9771	199.99	0.9751	198.63	0.9744	203.84	0.9747

TABLE-5
KINETIC STUDY OF PURE BLEND/SEBS/EPDM

Conversion	Differential method		Integral method				Average values	
	Friedman method		FWO method		KAS method			
	E_a (kJ/mol)	R^2	E_a (kJ/mol)	R^2	E_a (kJ/mol)	R^2	E_a (kJ/mol)	R^2
0.1	64.80065	0.9775	51.94448	0.9676	44.00093	0.9391	53.58	0.9533
0.2	81.12111	0.9788	58.85893	0.9692	50.94162	0.9412	63.64	0.9552
0.3	93.98254	0.9825	65.27423	0.9737	57.49081	0.9474	72.24	0.9606
0.4	110.7727	0.9752	71.6798	0.9649	64.05787	0.9354	82.17	0.9502
0.5	113.6666	0.9731	78.11809	0.9623	71.527	0.9321	87.77	0.9472
0.6	113.3811	0.9671	85.19606	0.9554	78.01384	0.9231	92.19	0.9393
0.7	120.4692	0.9655	90.50548	0.9536	83.48195	0.9206	98.15	0.9371
0.8	125.6945	0.9637	96.28805	0.9575	89.44783	0.9180	103.81	0.9378
0.9	211.4086	0.9714	103.6723	0.9604	97.08482	0.9296	137.38	0.9450
Average	115.03	0.972	77.94	0.962	70.67	0.931	87.88	0.947

this situation, while modelling the industrial processes, the average values might be used. The Friedman model offered slightly different results from the other two models, while the mathematical formulations of the FWO and KAS methods both permitted approximations.

The average activation energies for pure mix were 212.91, 199.99 and 198.63 kJ/mol. Nevertheless, the ternary pure blend showed the higher values for activation energy and the compatibilized blend, the values were 115.03, 77.94 and 70.67 kJ/mol. Since, the materials in a compatible mix are elastomeric in nature and hence require less energy for thermal breakdown, this may result in a decrease in the activation energy levels for all three of these models. While using the Friedman model, the values of E_a for pure blend suddenly changed from 0.1 to 0.3 and then the values showed a declined behaviour may be due to the build-up of volatiles over the surface of the specimen 0.6 to 0.7. The integral methods shows a stable range from 0.1 to 0.9. For low range conversion (0.1 to 0.2), there may be some undetected reaction that had occurred and in higher range, the temperature unfair distribution in the specimen is significant. There may have been an undetected reaction for the short range conversion and the specimen temperature unequal distribution is important for the high range conversion.

Thermal studies: TGA curves of pure blend and the blend with SEBS and EPDM are depicted in Fig. 7a-b. All the blends for pure and compatibilized ternary polymer blends demonstrated a single step degradation process. The low melting point and elastomeric nature of the compatibilizers reduce the thermal stability of blend. Since, the third carbon atom reduces the polymer stability, it is predicted that the pyrolysis temperature of PP will be less than that of HDPE. Compared to linear chain polymer like HDPE, branched and substituted polymers like PS and PP degrade at a lower temperature [26]. Therefore, the compatibilization has little impact on the ability of mixes to resist heat deterioration.

DSC curves of the pure uncompatibilized and compatibilized blends are shown in Fig. 8. A shift in the glass transition temperature was observed towards the lowest temperature,

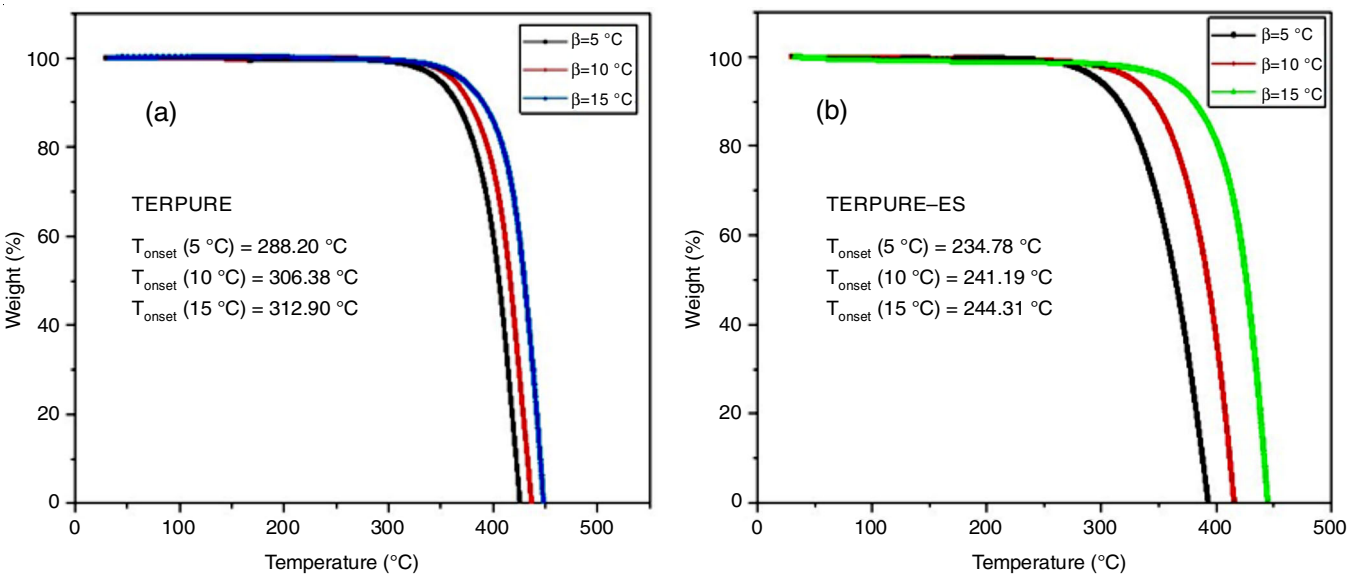

Fig. 7. TGA curves of (a) pure blend (b) pure blend with SEBS and EPDM

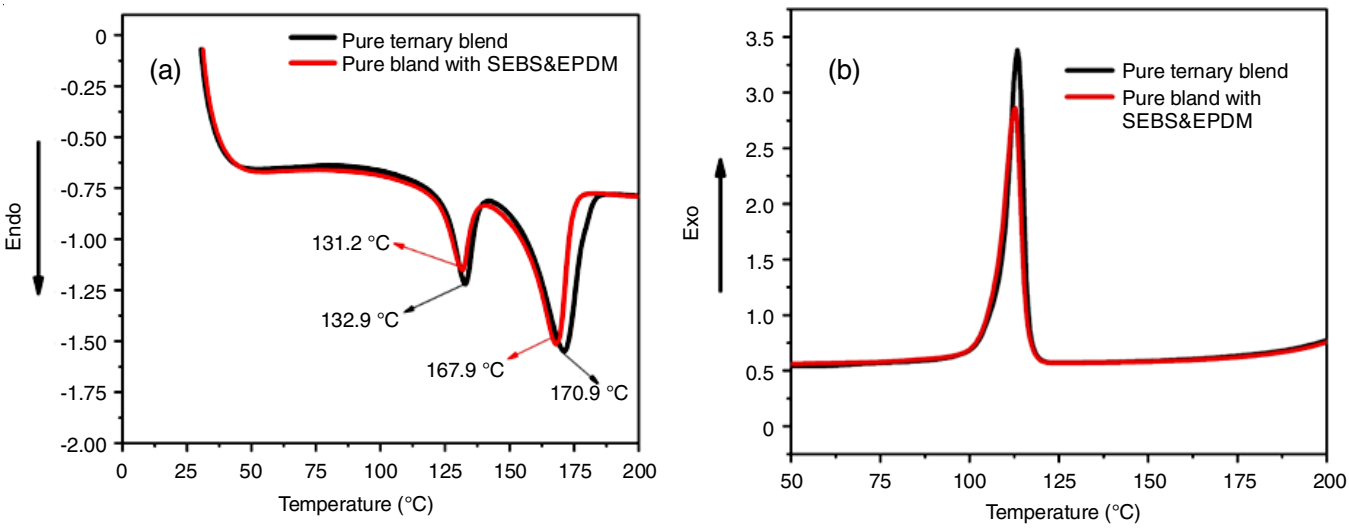

Fig. 8. DSC curves of (a) pure blend (b) pure blend with SEBS and EPDM

which confirmed the influence of SEBS and EPDM as compatibilizers in the PP/PS/HDPE ternary blends. This shift in the glass transition temperature can be due to the interaction of elastomeric SEBS and EPDM with the ternary polymer blend. This indicate that the blends can be used for the light weight automotive applications.

Morphological studies: Fig. 9 depicts the SEM images of pure and compatibilized polymer blends. The interfacial layers are easily seen in the morphology of pure blends (Fig. 9a-b) and it might be challenging to transmit stress uniformly between the layers. Therefore, surface cracks are easy to form, and compatibility of the polymer blend was visible. The formation of HDPE and PS in PP results in the phase separation inside the pure blend, which attributes a decline as a result of the non-uniformity in the stress distribution. The PS and HDPE were encapsulated in continuous phase by EPDM and SEBS in case of a compatible blend (Fig. 9c-d). Due to the compatibilizer in the blend, a significant reduction in the size of the dispersed phase is observed. The segment wise diffusion of EPDM blocks formed propylene into PP matrix and ethylene in HDPE droplets is a possible mechanism that can be seen in compatibilized blends. The EPDM elastomer migrates to interface during melt mixing and may form a layer over HDPE droplets, leading in the formation of an interpenetrated interface [27]. In case of SEBS, the styrene and ethylene blocks get attached with the similar branched part of the dispersed and continuous phase. The images clearly demonstrate that the system exhibits superior homogeneity and that HDPE and PS are easily compatible with EPDM and SEBS.

Flammability studies

Melt dripping characteristics: In polymer fires, dripping poses a serious concern. It may spread flames between distant objects and quicken their development. According to reports, interactions between the burning polymer and the pool fire encourage the spread of the fire and raise the risk of a fire by speeding up the burning and heat release rates. Whereas the random-chain scission breakdown mechanism often leads to the surface melting dripping, the end-chain scission decomposition mechanism corresponds to the bulk softening dripping

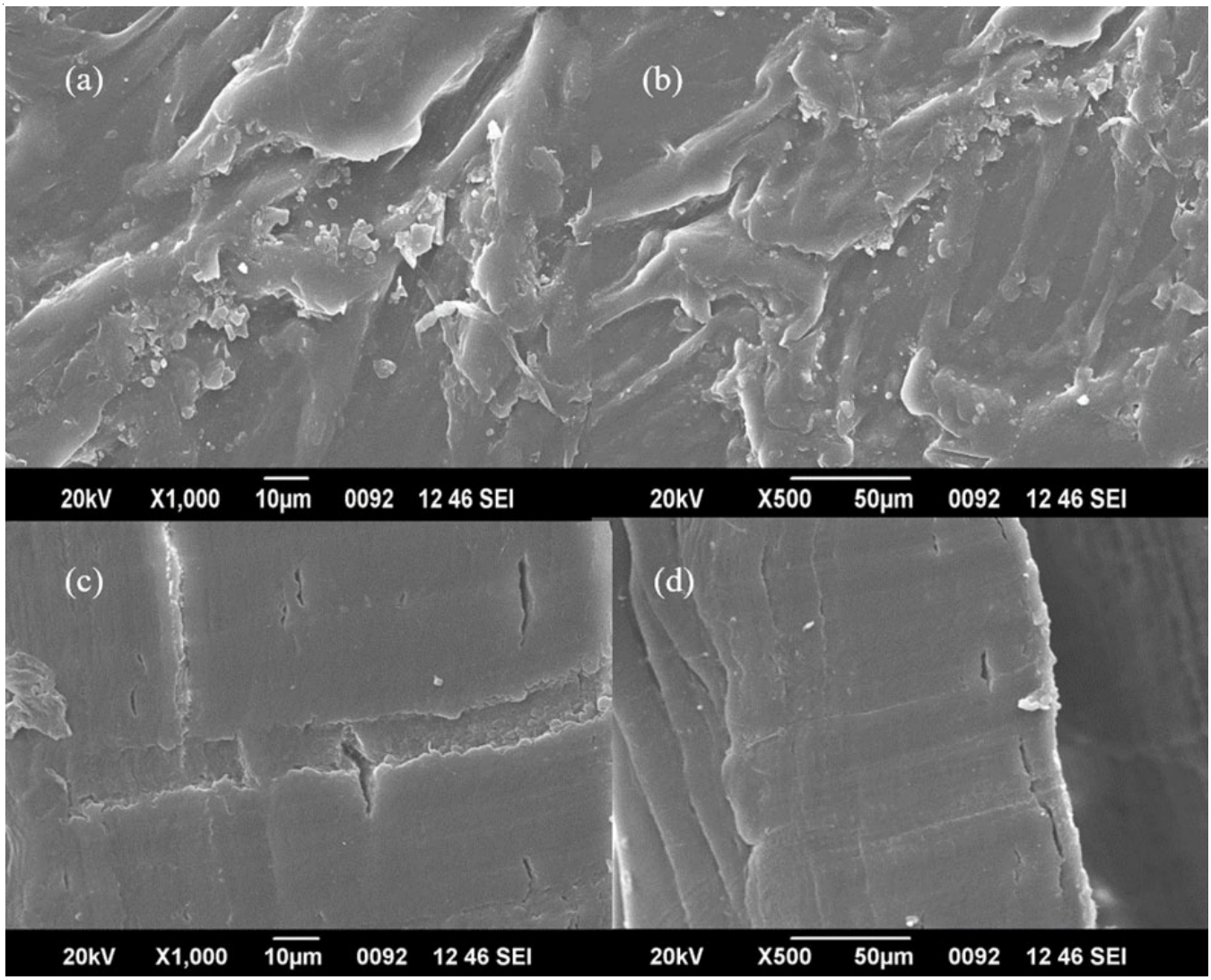

Fig. 9. SEM image of (a) pure ternary polymer blend at 10 µm (b) pure ternary polymer blend at 50 µm (c) compatibilized ternary polymer blend at 10 µm (d) compatibilized ternary polymer blend at 50 µm

type. The droplets that have been gathered resemble thin discs and most of the drops have branches at the terminal. This should be attributed to the splash of drops as they fell into the pan, suggesting that the viscosity of the drops at that time was low. Melt dripping study of the polymer blends were analyzed using the experimental setup is shown in Fig. 10a. The initial dripping times of the pure and compatibilized blends ranged from 15 to 20 s (Fig. 10b) and random-chain scission results in a sharp fall in the molecular weight, which lowers the viscosity. The compatibilized (PP/PS/HDPE/SEBS-EPDM) ternary blend had a faster time to ignition and initial dripping. The bond breakdown is accelerated by the decomposition mechanism, which also reduces the molecular weight where the dripping drop splashes on the bottom surface. With the sharp edges pointing outward and the narrow needle pattern, this creates a thin disk-shaped structure.

The time to ignition and initial dripping time were 9 s and 16 s for the pure blend and 6 s and 16 s for the compatibilized blends as indicated in Table-6. As observed a spherical droplets of a tiny diameter drip from a polymer specimen to an aluminium foil during the experimental research and the process continued to produce a piece of specimen drip at the end. In UL 94 test, both blends were not fallen under the categories mentioned by the test in ASTM. According to ASTM D2863, the limiting oxygen index (LOI) test was conducted to determine the flammability of organic polymers and composite materials. The most minimal amount of oxygen required to maintain burning combustion is known as LOI. The results are 18.4 and 18.3 for the pure and compatibilized blends, respectively. Due to the elastomeric character of the blend, which undoubtedly increases the flame, no such appreciable enhancement was observed in the composite material.

When the limiting oxygen index (LOI) of pure and compatible blends were examined, the results revealed no improvement in the flame resistance. The LOI results showed 18.7 and 18.9 since most of the composites comprised PP, PS, HDPE, SEBS and EPDM. Since, all the components are thermoplastic and elastomeric and thus are unable to withstand heat. The smoke and volatiles are generated through internal chain scission processes, which result in the degradation of the polymer chains.

Conclusion

The PP/PS/HDPE compatibilization was significantly improved by utilizing the ethylene-propylenediene-monomer (EPDM) and styrene-ethylene-butylene-styrene (SEBS) polymers. The enhancement in the mechanical characteristics further confirmed the impact of SEBS-EPDM in facilitating compatibility among the PP/PS/HDPE blends as demonstrated in the compatibility process. The interfacial agent between the polypropylene (PP) matrix and the dispersed PS/HDPE particles is made up of SEBS and EPDM polymers. It enhances the interfacial adhesion and reduces the interfacial tension. The findings also demonstrated that the interaction of elastomeric combinations of the compatibilizers enhanced tensile strength, tensile modulus and elongation at break. Three techniques were used to the investigate the activation energies for kinetic analysis. For Freidman, FWO and KAS methods, the average activation energies for pure blends (uncompatibilized) were 212.91 kJ/mol, 199.99 kJ/mol and 198.63 kJ/mol, whereas upon compatibilization, the values were found to be 115.03 kJ/mol, 77.94 kJ/mol and 70.67 kJ/mol, respectively. The low melting point and elastomeric makeup of the compatibilizers make the blend less thermally stable. A change in the glass transition temperature was observed, which indicates the compatibilization effect,

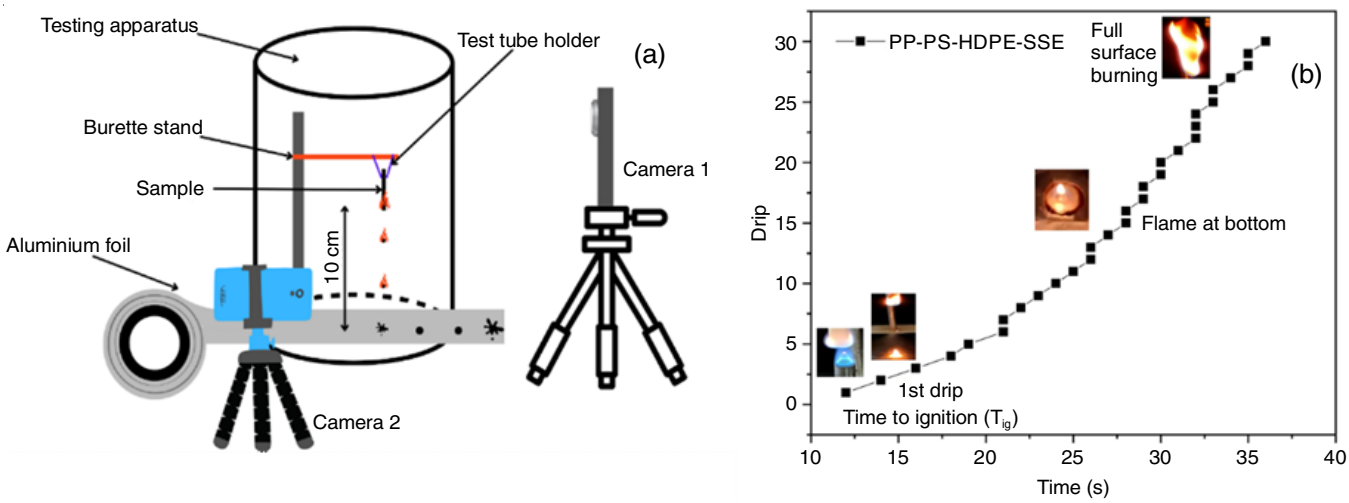

Fig. 10. Schematic representation of the setup used for melt dripping study (a) graphical representation of melt drip *versus* time (b)

TABLE-6
BURNING BEHAVIOUR CHARACTERISTICS OF PURE AND COMPATIBILIZED BLEND

Specimen	Time for sample to catch fire (s)	Time of drip start (s)	Total time for complete burning of sample (s)	Total number of drips	Maximum weight of drip (g)	Maximum diameter of drip (cm)
Pure blend	9	16	65	40	2.12	2.1
Compatibilized blend	6	15	57	47	1.59	2.4

according to DSC analysis. Due to the compatibilizer in the mixture, it has been shown that the size of the dispersed phase can be significantly reduced in morphological characterization. One probable process that might be observed in the compatible blends is the segment wise diffusion of EPDM blocks produced propylene into PP matrix and ethylene in HDPE droplets. The system is more homogeneous and HDPE and polystyrene are easily interchangeable with EPDM and SEBS. First dripping times for the pure and compatibilized blends were both under 15 s according to the melt dripping characteristics and random-chain scission causes molecular weight to decrease sharply and thereby reducing the viscosity. The fundamental mechanical characteristics of the compatibilizers indicate a considerable improvement with blending and at the same time, activation energies necessary for the reactions were also predicted. This demonstrates unequivocally that compatibilized blends are more resilient and efficiently transmit stress *via* the interface. It is possible to utilize this compatibilized blends in the low-temperature automotive applications.

CONFLICT OF INTEREST

The authors declare that there is no conflict of interests regarding the publication of this article.

REFERENCES

1. W. Brostow, T.H. Grguric, O. Olea-Mejia, D. Pietkiewicz and V. Rek, *E-Polymers*, **1**, 33 (2008); https://doi.org/10.1515/epoly.2008.8.1.355
2. M.O. Amankwa, E.K. Tetteh, G.T. Mohale, G. Dagba and P. Opoku, *Discov. Sustain.*, **2** 31 (2021); https://doi.org/10.1007/s43621-021-00040-z
3. N.R. Schwartz, A.D. Paulsen, M.J. Blaise, A.L. Wagner and P.E. Yelvington, *Fuel*, **274**, 117863 (2020); https://doi.org/10.1016/j.fuel.2020.117863
4. P. Palmay, C. Puente, D. Barzallo and J.C. Bruno, *Polymers*, **13**, 4379 (2021); https://doi.org/10.3390/polym13244379
5. I. Fortelný, Z. Kruliš, D. Michálková and Z. Horák, *Angew. Makromol. Chem.*, **270**, 28 (1999); https://doi.org/10.1002/(SICI)1522-9505(19990901)270:1<28::AID-APMC28>3.0.CO;2-U
6. J.M. Mendez, Ph.D. Thesis, Optimisation of the Mechanical Properties of HDPE/PP Blends and their Recyclable Composites, Cochin University of Science and Technology, Kochi, India (2009).
7. N. Vranjes and V. Rek, *Macromol. Symp.*, **258**, 90 (2007); https://doi.org/10.1002/masy.200751210
8. Y. Ding, C. Abeykoon and Y.S. Perera, *Adv. Ind. Manuf. Eng.*, **4**, 100067 (2022); https://doi.org/10.1016/j.aime.2021.100067
9. V. Thirtha, R. Lehman and T. Nosker, *Polymer*, **47**, 5392 (2006); https://doi.org/10.1016/j.polymer.2006.05.014
10. T.M. Kruse, S.E. Levine, H.W. Wong, E. Duoss, A.H. Lebovitz, J.M. Torkelson and L.J. Broadbelt, *J. Anal. Appl. Pyrolysis*, **73**, 342 (2005); https://doi.org/10.1016/j.jaap.2005.03.006
11. J. Briceno, M.A. Lemos and F. Lemos, *Int. J. Chem. Kinet.*, **53**, 660 (2021); https://doi.org/10.1002/kin.21472
12. Y. Li, Z. Qiang, X. Chen and J. Ren, *RSC Adv.*, **9**, 3128 (2019); https://doi.org/10.1039/C8RA08770A
13. K.P. Rajan, S.P. Thomas, A. Gopanna, A. Al-Ghamdi and M. Chavali, *Mater. Res. Express*, **5**, 085304 (2018); https://doi.org/10.1088/2053-1591/aad1d3
14. B. Spieß, E. Metzsch-Zilligen and R. Pfaendner, *Polym. Test.*, **103**, 107320 (2021); https://doi.org/10.1016/j.polymertesting.2021.107320
15. Y. Wang, F. Zhang, X. Chen, Y. Jin and J. Zhang, *Fire Mater.*, **34**, 203 (2010); https://doi.org/10.1002/fam.1021
16. Y. Wang, J. Jow, K. Su and J. Zhang, *J. Fire Sci.*, **30**, 477 (2012); https://doi.org/10.1177/0734904112446125
17. C.T. Hsieh, Y.J. Pan and J.H. Lin, *Fibers Polym.*, **18**, 155 (2017); https://doi.org/10.1007/s12221-017-6371-0
18. A.K. Goel, J. Kurek, G. Bartkowiak, D.O. Samson, E.K. Makama, H. Sutar, R. Murmu, C. Dutta, M. Ozcan, S.C. Mishra, V.A. Ryzhov, B.T. Melekh, M.A. Flores-Hidalgo, D. Barraza-Jiménez, D. Glossman-Mitnik and H.S. Min, *Adv. Mater. Sci. Eng.*, **1**, 105 (2019).
19. F.C. Chiu, H.Z. Yen and C.E. Lee, *Polym. Test.*, **29**, 397 (2010); https://doi.org/10.1016/j.polymertesting.2010.01.004
20. L.A. Al Juhaiman, D.A. Al-Enezi and W.K. Mekhamer, *Dig. J. Nanomater. Biostruct.*, **11**, 105 (2016).
21. F.C. Chiu, H.Z. Yen and C.C. Chen, *Polym. Test.*, **29**, 706 (2010); https://doi.org/10.1016/j.polymertesting.2010.05.013
22. S.E. Salih, A.F. Hamood and A.H. Abd Alsalam, *Modern Appl. Sci.*, **7**, 33 (2013); https://doi.org/10.5539/mas.v7n3p33
23. J. Parameswaranpillai, S. Jose, S. Siengchin and N. Hameed, *Int. J. Plast. Technol.*, **21**, 79 (2017); https://doi.org/10.1007/s12588-017-9172-9
24. X. Zhao, Y. Huang, M. Kong, Q. Yang and G. Li, *J. Appl. Polym. Sci.*, **135**, 46244 (2018); https://doi.org/10.1002/app.46244
25. S.A. Xu and C.M. Chan, *Polym. J.*, **30**, 691 (1998); https://doi.org/10.1295/polymj.30.691
26. R. Chen, X. Liu, L. Han, Z. Zhang and Y. Li, *Polym. Adv. Technol.*, **31**, 2722 (2020); https://doi.org/10.1002/pat.4998
27. J.H. Lin, Y.J. Pan, C.F. Liu, C.L. Huang, C.T. Hsieh, C.K. Chen, Z.I. Lin and C.W. Lou, *Materials*, **8**, 8850 (2015); https://doi.org/10.3390/ma8125496